Received: 8 May 2023 | Revised: 12 December 2023 | Accepted: 11 January 2024

https://doi.org/10.1016/j.jtha.2024.01.004

jth

ORIGINAL ARTICLE

Extracellular vesicles from activated platelets possess a phospholipid-rich biomolecular profile and enhance prothrombinase activity

Eduarda M. Guerreiro[1] | Sergei G. Kruglik[2] | Samantha Swamy[1] | Nadezhda Latysheva[1] | Bjarne Østerud[1] | Jean-Michel Guigner[3] | Franck Sureau[2] | Stephanie Bonneau[2] | Andrey N. Kuzmin[4] | Paras N. Prasad[4] | John-Bjarne Hansen[1,5] | Olav Gaute Hellesø[6] | Omri Snir[1,5]

[1]Thrombosis Research Group, Institute of Clinical Medicine, Univesitet i Tromsø - The Arctic University of Norway, Tromsø, Norway

[2]Laboratoire Jean Perrin, Institut de Biologie Paris-Seine, Sorbonne Université, Centre National de la Recherche Scientifique, Paris, France

[3]L'Institut de Minéralogie, de Physique des Matériaux et de Cosmochimie, Sorbonne Université, Centre National de la Recherche Scientifique, Institut de Recherche pour le Développement, Muséum National d'Histoire Naturelle, Paris, France

[4]Institute for Lasers, Photonics and Biophotonics and the Department of Chemistry, University at Buffalo, State University of New York, Buffalo, New York, USA

[5]Thrombosis Research Center, Division of Internal Medicine, University Hospital of North Norway, Tromsø, Norway

[6]Department of Physics and Technology, Univesitet i Tromsø- The Arctic University of Norway, Tromsø, Norway

Correspondence
Omri Snir, Thrombosis Research Group, Department of Clinical Medicine, Univesitet i Tromsø - The Arctic University of Norway, N-9037 Tromsø, Norway.
Email: snir.omri@uit.no

Sergei G. Kruglik, Laboratoire Jean Perrin, Institut de Biologie Paris-Seine, Sorbonne

Abstract

Background: Extracellular vesicles (EVs), in particular those derived from activated platelets, are associated with a risk of future venous thromboembolism.

Objectives: To study the biomolecular profile and function characteristics of EVs from control (unstimulated) and activated platelets.

Methods: Biomolecular profiling of single or very few (1-4) platelet-EVs (control/stimulated) was performed by Raman tweezers microspectroscopy. The effects of such EVs on the coagulation system were comprehensively studied.

Results: Raman tweezers microspectroscopy of platelet-EVs followed by biomolecular component analysis revealed for the first time 3 subsets of EVs: (i) protein rich, (ii) protein/lipid rich, and (iii) lipid rich. EVs from control platelets presented a heterogeneous biomolecular profile, with protein-rich EVs being the main subset (58.7% ± 3.5%). Notably, the protein-rich subset may contain a minor contribution from other extracellular particles, including protein aggregates. In contrast, EVs from activated platelets were more homogeneous, dominated by the protein/lipid-rich subset (>85%), and enriched in phospholipids. Functionally, EVs from activated platelets increased thrombin generation by 52.4% and shortened plasma coagulation time by 34.6% ± 10.0% compared with 18.6% ± 13.9% mediated by EVs from control platelets (P = .015). The increased procoagulant activity was predominantly mediated by phosphatidylserine. Detailed investigation showed that EVs from activated platelets increased the activity of the prothrombinase complex (factor Va:FXa:FII) by more than 6-fold.

Conclusion: Our study reports a novel quantitative biomolecular characterization of platelet-EVs possessing a homogenous and phospholipid-enriched profile in response to platelet activation. Such characteristics are accompanied with an increased

Manuscript handled by: Patricia Liaw

Final decision: Patricia Liaw, 11 January 2024

© 2024 The Author(s). Published by Elsevier Inc. on behalf of International Society on Thrombosis and Haemostasis. This is an open access article under the CC BY license (http://creativecommons.org/licenses/by/4.0/).

Université, Centre National de la Recherche Scientifique, 75005 Paris, France.
Email: sergei.kruglik@sorbonne-universite.fr

Funding information
This work was supported by the North Norwegian Regional Health Authority (grant HNF1548-20 to O.S.). A.N.K. and P.N.P. at the Institute for Lasers, Photonics, and Biophotonics acknowledge support from the office of the vice president for research and economic development at the University at Buffalo.

phosphatidylserine-dependent procoagulant activity. Further investigation of a possible role of platelet-EVs in the pathogenesis of venous thromboembolism is warranted.

KEYWORDS
biomolecular composition, platelet extracellular vesicles, prothrombinase activity, Raman tweezers microspectroscopy, venous thromboembolism

1 | INTRODUCTION

Venous thromboembolism (VTE), a collective term (thrombosis and embolism) for deep vein thrombosis and pulmonary embolism, is a complex disease with severe short- and long-term complications, including death [1,2]. Growing evidence indicates that platelet activation plays an essential role in the pathogenesis of VTE [3,4]. High mean platelet volume, a measure of increased platelet activation [5], as well as high levels of von Willebrand factor, are associated with the risk of future VTE [6–8], while inhibition of platelet activation reduces the risk of recurrent VTE [3]. Recently, we reported that elevated levels of platelet-derived extracellular vesicles (platelet-EVs) in plasma were associated with risk of future development of VTE [9]. The association was driven by EVs derived from activated platelets, which suggests a role for platelet activation and subsequent release of platelet-EVs in the pathogenesis of VTE.

Platelet activation leads to exposure of negatively charged phospholipids (phosphatidylserine [PS] and phosphatidylethanolamine [PE]) on their membrane outer leaflet [10]. A "cap"-like bowed region on the activated platelet membrane enriched with PS can bind coagulation factors II, V/Va, VIII, IX, and X, serving as a surface for assembly and activation of the intrinsic tenase (FVIIIa, FIXa, and FX) and prothrombinase complexes (FVa, FXa, and FII) [11]. The composition of phospholipids and proteins on the surface of platelet-EVs, however, differs from the platelet membrane [12]. Still, platelet-EVs display high levels of negatively charged phospholipids on the outer leaflet of their membrane [13], and variation in the composition of phospholipids on the outer surface of platelet-EVs affects the assembly of coagulation factors on the platelet-EV membrane [14] and thus their procoagulant activity. Of note, it has been reported that EVs from activated platelets bear high procoagulant activity, which was estimated to be 50-100 times higher than the procoagulant activity of platelets [15]. These observations suggest that platelet-EVs, and particularly those derived from activated platelets, play a major role in coagulation processes. As a substantial number of EVs detected in plasma are derived from platelets [16,17], and as levels of such EVs are increased in different pathological conditions [9,18,19], a detailed investigation of the role of platelet-EVs in coagulation is of particular interest.

In this work, we studied in detail the biomolecular composition of EVs from control (unstimulated) and activated platelets and their effect on the coagulation cascade. Raman tweezers microspectroscopy (RTM) was employed as it provides detailed information regarding the biochemical composition of single or very few EVs [20–22]. Recently, label-free characterization of single EVs in blood has been performed by synchronous Rayleigh and Raman scattering, also employing optical traps [23,24]. In contrast to these studies, our current work was devoted to a detailed characterization of EVs derived from isolated platelets in order to avoid complications due to the complex environment in whole blood. Our analysis revealed for the first time 3 principal subsets of platelet-EVs, distinguished by their content of proteins and lipids. While the majority of EVs and possibly other extracellular particles from control platelets were enriched with proteins, a biomolecular shift toward a phospholipid-rich composition was found for EVs from activated platelets. This shift was associated with an increased procoagulant activity, mediated specifically via the prothrombinase complex.

2 | MATERIALS AND METHODS

2.1 | Platelet activation and isolation of platelet-derived EVs

Collection of clinical samples has been approved by the regional Ethical Committee for Medical and Health Research Ethics (REK80025). All participants were above the age of 18 years (Table 1) and did not suffer from illness or used medication; all gave written informed consent. Blood was drawn by venipuncture of the antecubital vein using a 21-gauge needle and minimal stasis. Blood was collected into Vacuette 6 mL Z tubes with no additives (Greiner Bio-One); the first tube was discarded. Acidic citrate dextrose buffer (39 mM citric acid, 75 mM sodium citrate, 135 mM [D]-glucose, pH 4.5) and 2.8 mM Prostaglandin E1 (PGE1, MedChemExpress) were added rapidly to the blood to prevent blood coagulation and platelet activation, respectively. Additional 3 mL of blood was drawn into K2EDTA Vacuette tubes (Greiner Bio-One) for cell count using an ABX

TABLE 1 Basic information of the donors participating in the study.

Participants	9	
Age (y), mean ± SD	39.9 ± 7.2	
Sex (%)	Male	55.5
	Female	45.5

MicrosES60 (ABX Diagnostics). Following addition of acidic citrate dextrose buffer and PGE1, blood was centrifuged at 140 ×g for 15 minutes with no breaks (room temperature) using a Megafuge 1.0 (Heraeus Sepatech) centrifuge equipped with a swing bucket rotor BS4402/A to generate platelet-rich plasma. Platelet pellets were recovered from platelet-rich plasma following centrifugation at 900 ×g for 15 minutes at room temperature, washed twice with HEPES-NaCl buffer (10 mM HEPES, 145 mM NaCl, pH 7.4) and 2.8 mM PGE1, and resuspended in Tyrode-HEPES buffer (10 mM HEPES, 145 mM NaCl, 1 mM $MgCl_2$, 2 mM $CaCl_2$, 3 mM KCl, pH 7.4). Platelets (250×10^6 in 1 mL Tyrode-HEPES buffer) were stimulated with 100 μM thrombin receptor activator peptide 6 (TRAP-6, MedChemExpress) or 2 μM calcium ionophore A23187 (Sigma-Aldrich) for 15 minutes at 37 °C. Saline was added for time-matched unstimulated control platelets. Following the 15-minute incubation, EDTA was added to platelet suspensions (activated and time-matched control) at a final concentration of 10 mM to held platelet activation. Platelets were sedimented at 2500 ×g for 10 minutes at room temperature. Supernatant was transferred to a new tube before proceeding with isolation of platelet-EVs, and the platelet pellets were resuspended in 1% paraformaldehyde in phosphate buffered saline for assessment of platelet activation by flow cytometry (see Supplementary methods for details). Platelet-derived (micro)particles, hereafter referred to as platelet-EVs, were isolated from supernatant by centrifugation at 20,000 ×g for 30 minutes at 4 °C, using a 5810R Eppendorf centrifuge with a fixed angle rotor FA-45-30-11. EV pellets were resuspended in 1/10 of their initial volume (ie, 10× concentrated) in a buffer suitable for the respective downstream analysis. For EV characterization by Raman spectroscopy, nanoparticle tracking analysis, and cryogenic transmission electron microscopy (Cryo-TEM), EV pellets were resuspended in phosphate buffered saline. For analysis of procoagulant activity of EVs by procoagulant phospholipid (PPL) clotting assay and thrombin generation by calibrated automated thrombogram (CAT), EVs were resuspended in pooled EV-depleted plasma (EVDP). EVDP was prepared as previously described by Ramberg et al. [25]. Briefly, citrated blood from 10 healthy individuals was centrifuged twice at 2500 ×g to produce platelet-free plasma, which was subjected to ultracentrifugation (100,000 ×g, 60 minutes) at 16 °C (Beckman Optima LE-80 K Ultracentrifuge, rotor SW40TI, Beckman Coulter). EVDP samples were pooled, aliquoted, and stored at −80 °C until further use.

For analysis of the prothrombinase complex activity, EVs were resuspended in 20 mM HEPES/150 mM NaCl buffer. All EV suspensions were stored at −80 °C until use.

2.2 | Enumeration and size distribution of platelet-EVs

Particle concentration and size distribution were determined using a NanoSight NS300 (Malvern Instruments Ltd) using a 488 nm blue laser and a CMOS camera. Platelet-EVs were diluted (100×) prior to analysis, loaded using a syringe, and captured at room temperature. For each sample, 5 movies of 60 seconds each were recorded, refreshing the sample between captures, and analyzed using the Nanoparticle Tracking Analysis software (v.3.3 Dev Build 3.3.301). Camera level was set to 14 and detection threshold to 5.

2.3 | Cryo-TEM

Cryo-TEM images of EVs were obtained using the protocol reported elsewhere [20,21]. Briefly, 4 μL droplet of aqueous suspension with the highest available EV concentration (particles' concentration ranged from 10^{10} to 10^{12} mL^{-1}) was deposited on a holey carbon grid (Quantifoil, Quantifoil Micro Tools GmbH). Excess liquid on the grid was absorbed with a filter paper. Simultaneously, the grid was rapidly plunged into liquid ethane to form a thin, homogenous vitreous ice film using a specially designed *ad hoc* appliance. The vitrified sample was then placed in a liquid-nitrogen-cooled cryo-holder (Gatan 626, Gatan Inc), transferred into the side microscope entry, and studied at low temperature (−180 °C). Cryo-TEM images were recorded with a 2k × 2k CCD camera (Gatan Ultrascan 1000, Gatan Inc) using a transmission cryo-electron microscope operating at 200 kV (LaB6 JEOL JEM2100, JEOL Ltd). A special low-dose system (Minimum Dose System, JEOL Ltd) was used to protect thin vitreous ice film from irradiation before imaging and to reduce irradiation during image recording. Representative Cryo-TEM images used to verify the presence of double-membrane EVs in all our samples are shown in Supplementary Figure S1B.

2.4 | Raman tweezers microspectroscopy

Raman spectra were recorded using the in-house built RTM setup described elsewhere [20,21], with several modifications. Briefly, continuous-wave near-infrared excitation light at 780 nm with an average power of ∼180 mW at the sample position was provided by a Ti:Sapphire laser (Model 3900S, Spectra-Physics) pumped by a DPSS laser (Millennia eV, Spectra-Physics) delivering 2.3 W at 532 nm. The 780 nm light was used for both optical trapping of EVs in water suspension and excitation of Raman scattering from them using a long working distance water-immersion infinity-corrected objective (Olympus LUMFL, magnification = 60×, numerical aperture = 1.1). The upright microscope configuration was implemented with the objective lens directly plunged into the aqueous sample containing EVs with a typical volume of ∼120 μL. The focal point was located approximately 2 mm above the stage slide made of CaF_2.

Raman scattering from all the biomolecules within the optical trap was collected in a backscattering geometry, spectrally filtered off with a

pair of beamsplitters plus a long-pass filter (Semrock RazorEdge, grade "U"), and focused onto the 50-μm spectrometer entrance slit using a 75-mm achromatic focusing lens. For Raman spectrum detection, an optical spectrometer was used having a 500-mm focal length with a 400 lines/mm grating optimized for 850 nm (Acton SpectraPro 2500i, Princeton Instruments), in combination with a deep-depletion back-illuminated near-infrared CCD detector (SPEC-10 400BR/LN, Princeton Instruments), cooled down to 140 °K using liquid nitrogen.

Raman spectra were acquired using the WinSpec/32 (Princeton Instruments) software. One experimental run consisted of 100 sequentially recorded spectra with an accumulation time of 3 seconds per spectrum. Concerning the "single-vesicle" regime of trapping, the amount of EVs within an optical trap depends on experimental conditions (nanoparticle size, concentration, biomolecular composition, measurement time, etc.); a detailed discussion of this question can be found in an earlier work by Kruglik et al. [21]. In the present study, the EV concentrations for the RTM experiment was in the range 1.8×10^9 to 2.0×10^{10} mL^{-1}, depending on the sample. From the analysis of the events of sequential abrupt intensity, increase with time in the recorded Raman spectra, Raman intensity normalization on the water band at ~1640 cm^{-1}, and calculation of the ~1440 cm^{-1} band area arising from $CH_{2,3}$ deformations of proteins and lipids (Supplementary Figure S2), we estimated the amount of trapped EVs to be within the range from 1 to 4 in a random fashion in 1 experimental run. The precise number of trapped bioparticles is difficult to determine in the case of multiparticle trapping because of substantial variability in particle size and biomolecular content; Supplementary Figure S3 provides our best possible estimate. The analysis of the Raman signal from such a low number of trapped EVs is the closest approximation to biochemical analysis at the single-vesicle level, as opposed to bulk analysis, averaging the signal from multiple particles.

2.5 | Raman data pretreatment and biomolecular component analysis

The initial Raman data treatment was performed using the IgorPro for Windows software (Wavemetrics); it consisted of frequency calibration using toluene lines, subtraction of water background, spectra averaging, and correction of slowly changing residual background using a polynomial function.

Further quantitative analysis of the corrected Raman spectra was performed using biomolecular component analysis (BCA) as previously described [26–29]. In our study, the analysis involved decomposition of the recorded Raman spectrum of EVs into predetermined spectral components using the nonlinear least-squares solver *lsqcurvefit* in MATLAB R2022a software (MathWorks). Each spectral component represents the contribution from a particular general class of biomolecules; their initial choice was based on the experience of using BCA for Raman imaging of organelles in living cells [28,29]. Further fine-tuning was performed iteratively, optimizing the shape of the protein spectrum and adding the carotenoid contribution. Supplementary Figure S4 shows all 15 biomolecular spectral components used in this work. In addition, special routines were used to model the C=C cis-trans transition in the 1645-1670 cm^{-1} range, the variability of the C=O band position within the 1710-1750 cm^{-1} range for lipids, and also the variability of the C=C band position in 1510-1540 cm^{-1} for carotenoids. Supplementary Figure S5 illustrates the decomposition of the measured Raman spectrum (after initial treatment, see above) into the model biomolecular spectral components (Supplementary Figure S4) in the experimental run with a single (Supplementary Figure S5A) and a few (most probably 3) (Supplementary Figure S5B) trapped bioparticles. Supplementary Figure S6 presents examples of Raman spectra fitting using BCA for EVs from 1 donor at all 3 platelet states (control, TRAP-6-activated, and A23187-activated), showing the biomolecular contributions from all lipids and proteins, together with the residual traces after spectral fitting.

2.6 | Measurements of thrombin generation in plasma by CAT

Thrombin generation in plasma was measured using CAT as previously described [30,31]. EVs from control or activated platelets were used as the source of phospholipids. Forty microliters of concentrated platelet-EVs in EVDP (10×) were mixed with 10 μL of 6 pM relipidated recombinant human tissue factor (TF) (Dade Innovin, Siemens Healthcare) and 50 μL of 20 mM HEPES/140 mM NaCl buffer in a U-bottom well of a 96-well microtiter plate (Immulon, Lab Consult). Fluorescence intensity was detected at 460 nm (emission filter) and 355 nm (excitation filter).

2.7 | PPL clotting assay

PPL-dependent clotting assay was performed using a Start Max instrument from Diagnostica Stago, as previously described [25], with minor adjustments. Briefly, EVs isolated from 250×10^6 platelets/mL were reconstituted in 500 μL EVDP (ie, 2×). Fifty microliters of EV/EVDP suspension were loaded to a Start-cuvette (Diagnostica Stago) with a steel ball and incubated for 2 minutes at 37 °C. Clotting was initiated with the addition of 100 μL of prewarmed FXa reaction buffer (bovine FXa [bFXa] 0,1 U/mL, Enzyme Research Laboratory, 15 mM $CaCl_2$, 100 mM NaCl, 20 mM HEPES, pH 7.0) and clotting time was registered. All samples were tested in duplicate. The mean coagulation time was used for further analysis. Clotting time of EVDP ($EVDP_{CT}$) was arbitrarily assigned as 100%. Decreased clotting time was converted to a procoagulant activity (in percentage). The changes in procoagulant activity were calculated as follows: 100% (EVDP) + $[(EVDP_{CT} - EV_{CT})/(EVDP_{CT})] \times 100$.

To examine the role of PS and PE displayed by platelet-EVs in plasma coagulation, as measured by PPL assay, platelet-EVs were preincubated with PS and PE-specific blockers, ie, lactadherin (Prolytix) and duramycin (Sigma Aldrich), respectively. Increased amounts of lactadherin (5, 10, 20, 40, and 80 nM) or duramycin (4, 8, 16, and 32 μM) were added to platelet-EVs and incubated for 30 minutes on ice. Clotting assay was performed as described above.

2.8 | TF-dependent thrombin generation assay in the presence of platelet-EVs

The ability of platelet-EVs to support TF activity was tested using a modification of a TF-dependent thrombin generation assay [32]. Platelet-EVs were used as the source of phospholipids (UPTT Reagent was omitted from reaction). Concentrated platelet-EVs were diluted to 2×. EV suspension from control or TRAP-6-activated platelets (30 μL) was added to 15 μL relipidated recombinant human TF (final concentration 500 fM) and 30 μL of a coagulation mix containing human coagulation FII, FX, FVIIa, and bFV/Va (all from Enzyme Research Laboratories) with final concentrations of 260 nM, 37.6 nM, 68 pM, and 571.2 mM, respectively. The mixture was preincubated at 37 °C for 5 minutes and the reaction was initiated with the addition of 15 μL prewarmed 50 mM $CaCl_2$ in 20 mM HEPES/150 mM NaCl buffer. After 4 minutes of incubation at 37 °C, 30 μL of 2.5 mM thrombin-specific chromogenic substrate (Spectrozyme TH, Sekisui Diagnostics) was added. Following 5 minutes at 37 °C, the reaction was halted with 50 μL of a buffer solution pH 4.0 (Certipur) and optical density (OD) was read at 405 nm using a MultiScan FC plate reader (Thermo Fisher Scientific). Samples were analyzed in duplicate.

2.9 | Prothrombinase complex activity assay

To study the effects of platelet-EVs on the prothrombinase complex activity, concentrated EVs from control and TRAP-6-activated platelets were diluted to 2× in 20 mM HEPES/150 mM NaCl buffer. Platelet-EVs (30 μL) were mixed with 30 μL of a mixture of bFXa, bFV/Va, and human FII with final concentrations of 22.4 nM, 185 nM, and 158 nM, respectively. To initiate thrombin generation, 15 μL of prewarmed 50 mM $CaCl_2$/20 mM HEPES/150 mM NaCl buffer was added. Following 4 minutes at 37 °C, 30 μL of 2.5 mM thrombin-specific chromogenic substrate (Spectrozyme TH, Sekisui Diagnostics) was added and incubated for 5 minutes. The reaction was quenched with 50 μL buffer solution pH 4.0 (Certipur). OD was determined using MultiScan FC plate reader at 405 nm wavelength. Samples were analyzed in duplicate.

To assess the effect of PS and PE expressed on platelet-EVs on the activity of the prothrombinase complex, platelet-EVs were preincubated with 2.5, 5, 10, and 20 nM lactadherin or 100, 250, 500, and 1000 nM duramycin for 15 minutes at room temperature prior to the addition of the mixture of the coagulation factors.

2.10 | Statistical analysis

One-way analysis of variance (Kruskal–Wallis test) followed by Tukey's multiple comparison test were used to analyze the differences between groups using GraphPad Prism v.9.2.0 (GraphPad Software). *P* values < .05 were considered significant. Paired *t*-test was used for comparison between groups in CAT.

3 | RESULTS

3.1 | EVs from activated platelets display a stabilized lipid and protein-rich biomolecular profile

Biomolecular profiles of EVs from control platelets and platelets activated with either TRAP-6 or calcium ionophore (A23187) were analyzed using RTM, a technique suitable to obtain information on the biomolecular composition of EVs in the optical trap [20–22]. Representative Raman spectra of a single or a very small number of EVs from control and activated platelets are presented in Figure 1A. Next, BCA was performed on the acquired spectra, focusing on the proteins/lipids concentration ratio carried by platelet-EVs. As depicted in Figure 1B, this analysis revealed 3 distinctive subsets of platelet-EVs: (i) protein-rich EVs (zone A), (ii) EVs that are rich in both proteins and lipids (zone B), and (iii) lipid-rich EVs (zone C). Importantly, BCA revealed little triglycerides and cholesterol in the sample associated with lipoproteins [33], thus providing an indication for low contamination of lipoproteins. EVs from control platelets displayed a large spread of proteins-to-lipids ratio, with protein-rich EVs being the dominating species (50%-72%, Figure 1B, zone A, Table 2). Smaller fractions of EVs from control platelets were rich with both proteins and lipids (17%-32%, zone B) or predominantly lipid-rich (3%-18%, zone C). In contrast, EVs from TRAP-6-activated platelets exhibited a more homogenous biomolecular distribution, with the dominant species being rich with both proteins and lipids (72%-90%, Figure 1B, Table 2); marginal fractions showed protein- (3%-13%) or lipid-rich (0%-21%) profiles. This behavior was accentuated following platelet activation with calcium ionophore, as 93% to 100% of EVs were rich with both proteins and lipids, and 7% of EVs were lipid-rich. Taken as a whole, data show that the biomolecular profile of EVs from activated platelets differs from that of EVs from control platelets.

Of note, the relative concentration of phospholipids within the trapped EVs, analyzed by BCA, showed that EVs from TRAP-6 and calcium ionophore–activated platelets carry higher amounts of phospholipids in comparison with EVs from control platelets (Figure 1C).

3.2 | Increased procoagulant activity of EVs from activated platelets

The increased amount of phospholipids detected on EVs from activated platelets prompted us to compare the characteristics and procoagulant activity of EVs from control and activated platelets. Similar to previous reports [34], no significant differences in the quantity of particles collected from control or TRAP-6-activated platelets were observed (Figure 2A, B). The number of EVs isolated from platelets activated with calcium ionophore, however, increased significantly (Figure 2A, B). EVs from control platelets had an average mode particle size of 115.6 ± 38.6 nm (Figure 2C). In comparison, EVs derived from platelets activated with TRAP-6 and calcium ionophore had a mode particle size of 161.7 ± 32.6 nm and 160.2 ± 20.7 nm, respectively (Figure 2C).

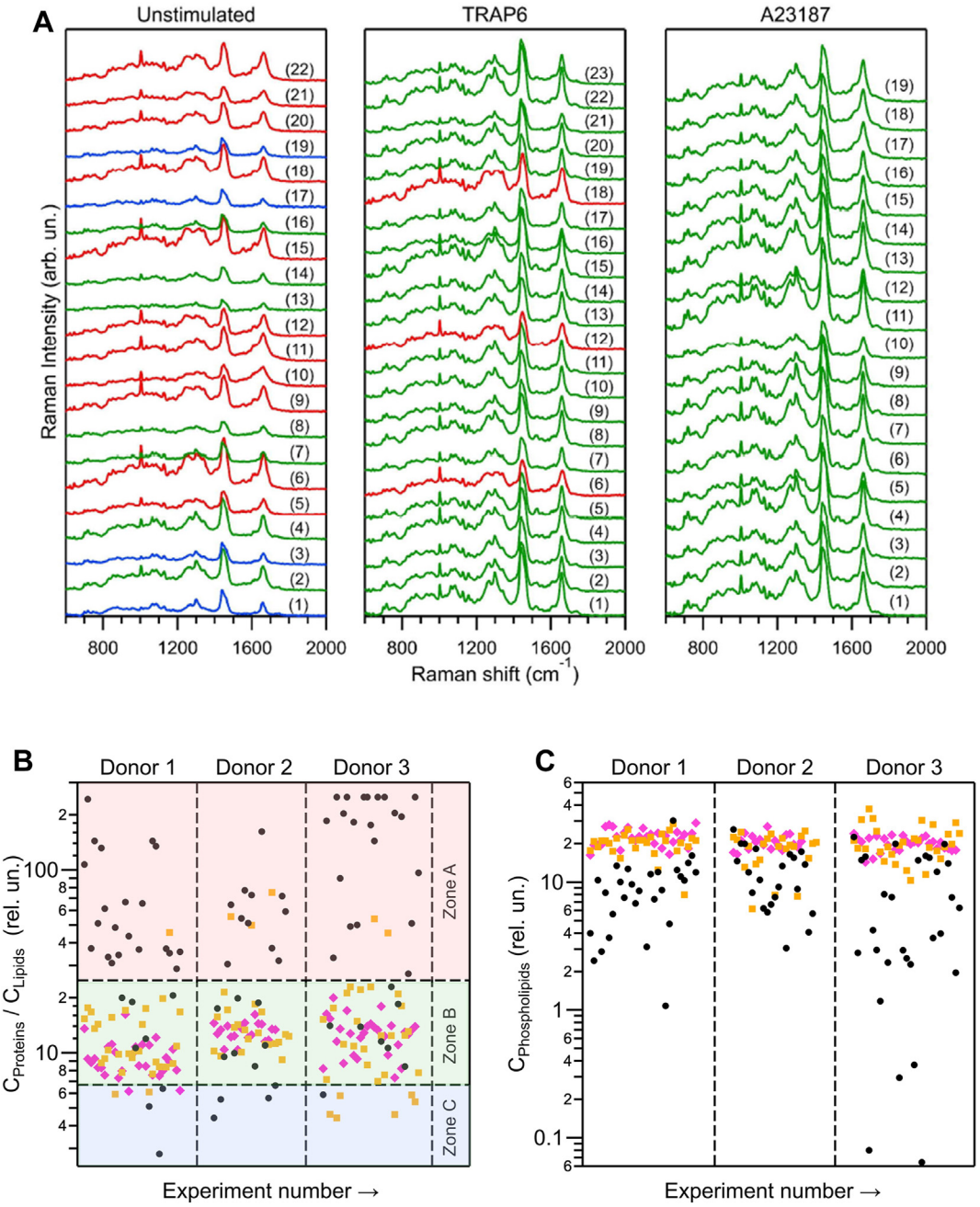

FIGURE 1 (A) Representative recorded Raman spectra of optically trapped extracellular vesicles (EVs) after initial data processing for donor 2. Left subpanel: spectra of EVs from control platelets; middle subpanel: thrombin receptor activator peptide 6 (TRAP-6) activated platelets; and right subpanel: A23187 (calcium ionophore) activated platelets. The sequential number of each Raman experiment is indicated in parentheses to the right of the corresponding spectrum. Red-colored spectra: protein-rich EVs; green-colored spectra: EVs with a large contribution from both protein and lipids; blue-colored spectra: lipid-rich EVs. (B) Relative protein-to-lipid concentration ratio following biomolecular component analysis of the acquired Raman spectra for all 3 donors. Zone A: EVs with dominant protein contribution and minor or negligible lipids contribution; zone B: EVs with variable non-negligible contribution of both proteins and lipids; zone C: EVs dominated by lipids and very little protein content. (C) Relative concentration of phospholipids normalized on the number of trapped EVs following biomolecular component analysis of the recorded Raman spectra for all 3 donors. In panels (B) and (C), each data point corresponds to 1 experimental run with an EV-trapping event. Black circles: EVs from control platelets; yellow boxes: TRAP-6-activated platelets; magenta rhombs: A23187 (calcium ionophore)-activated platelets.

Although calcium ionophore is commonly used to study platelet activation [35,36], it is a nonphysiological agonist of platelets [37] that induces a vigorous platelet response. As calcium ionophore increased the generation of platelet-EVs by 10-fold (Figure 2B) in comparison with control and TRAP-6-activated platelets, and as platelet activation with calcium ionophore is not physiologically relevant [38], EVs from platelets stimulated with this agonist were not included in further analysis.

print & web 4C/FPO

TABLE 2 Distribution of the biomolecular profile of extracellular vesicles derived from control platelets, platelets activated with TRAP-6, and platelets activated with calcium ionophore (A23187).

	Control (unstimulated)			TRAP-6			Calcium ionophore (A23187)		
	Donor 1 (%)	Donor 2 (%)	Donor 3 (%)	Donor 1 (%)	Donor 2 (%)	Donor 3 (%)	Donor 1 (%)	Donor 2 (%)	Donor 3 (%)
Protein-rich (zone A)	72.4	50.0	72.4	3.4	13.0	6.9	0.0	0.0	0.0
Proteins and lipids (zone B)	17.2	31.8	24.1	89.7	87.0	72.4	93.1	100.0	100.0
Lipid-rich (zone C)	10.3	18.2	3.4	6.9	0.0	20.7	6.9	0.0	0.0

TRAP-6, thrombin receptor activator peptide 6.

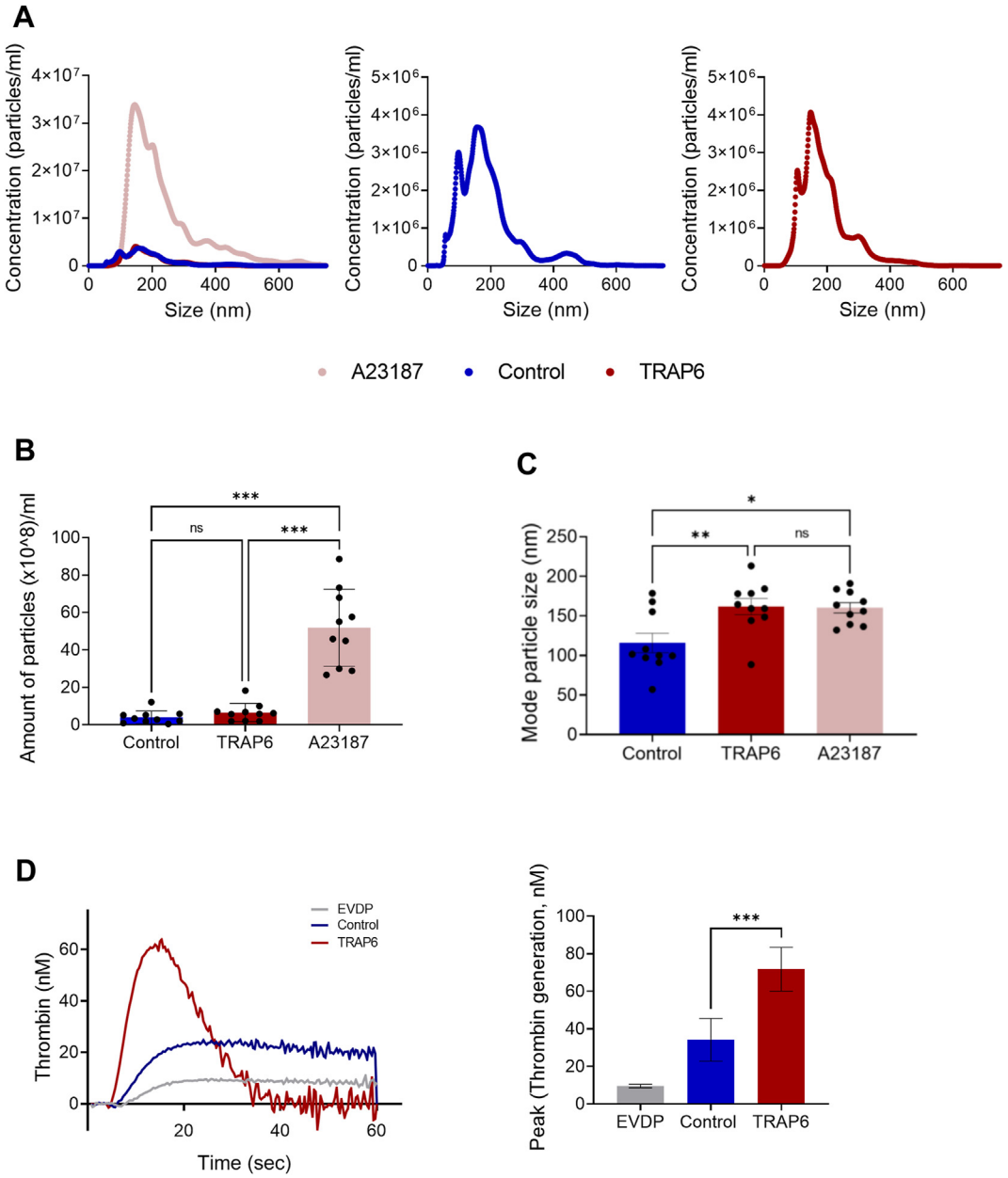

FIGURE 2 (A) Particle size distribution (n = 5), (B) concentration (n = 10), and (C) mode particle size (n = 10) of extracellular vesicles (EVs) from control platelets, platelets activated with thrombin receptor activator peptide 6 (TRAP-6), or calcium ionophore (A23187), assessed by nanoparticle tracking analysis. (D) Representative curve of thrombin generation in EV-depleted plasma (EVDP) following addition of EVs derived from control and TRAP-6-activated platelets as the source of phospholipids (left-hand panel). EVs derived from TRAP-6-activated platelets support thrombin generation (n = 3, middle panel) and Peak (thrombin generation) (n = 3, right-hand panel) in a more efficient manner in comparison to the EVs from control platelets. *P < .05, **P < .01, ***P < .0005.

print & web 4C/FPO

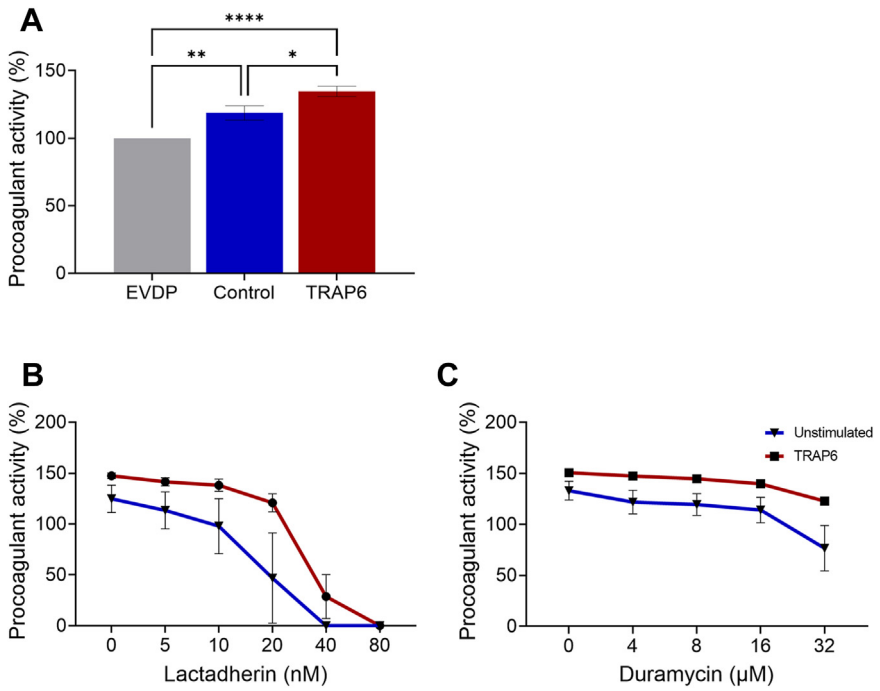

FIGURE 3 (A) Extracellular vesicles (EVs) were isolated from control and thrombin receptor activator peptide 6 (TRAP-6) activated platelets of healthy subjects (n = 7) and added to EV-depleted plasma (EVDP). The clotting time of EVDP only or EVDP supplemented with platelet-EVs was measured using a procoagulant phospholipid factor Xa-dependent coagulation assay. Reduced clotting time following the addition of platelet-EVs is presented as increased procoagulant activity. Clotting time of EVDP was set as 100%. The effects of (B) phosphatidylserine and (C) phosphatidylethanolamine displayed by platelet-EVs on plasma coagulation were assessed. EVs from control platelets or platelets activated with TRAP-6 were treated with increased concentrations of lactadherin or duramycin to block phosphatidylserine or phosphatidylethanolamine, respectively. Lactadherin (B) or duramycin (C) treated platelet-EVs were added to EVDP, and the procoagulant activity was determined using a procoagulant phospholipid FXa-dependent coagulation assay (n = 3). $^{*}P < .05$, $^{**}P < .005$, $^{***}P < .0001$.

print & web 4C/FPO

Next, the procoagulant activity of EVs isolated from control and TRAP-6-activated platelets was compared using CAT, which monitors the physiological dynamics of coagulation activation assessed by thrombin generation over time. Addition of EVs from activated platelets to EVDP resulted in higher thrombin generation (peak) in comparison with addition of EVs from resting platelets (Figure 2D). Thrombin generation was dependent on the amount of platelet-EVs added to the reaction (Supplementary Figure S7A).

3.3 | The procoagulant activity of platelet-EVs is mediated primarily by PS

Next, we assessed the effects of EVs from control and activated platelets on the final steps of the coagulation system, which involve the prothrombinase complex and the generation of thrombin using a PPL FXa-dependent assay [31]. EVs from control and activated platelets were added to EVDP. Clotting was initiated with the addition of extrinsic FXa, and the clotting time was recorded; the clotting time of EVDP was set to 100%. The reduced clotting time following addition of platelet-EVs was interpreted as an increased procoagulant activity. As shown in Figure 3A, EVs from control platelets increased the procoagulant activity by 18.6% ± 13.9%. The procoagulant activity following addition of EVs from TRAP-6-activated platelets to EVDP increased by 34.6% ± 10.0%. The increased activity was dose-dependent (Supplementary Figure S7B).

PS and PE displayed on the surface of platelet-EVs facilitate the assembly and activity of several coagulation factors [39]. To test the involvement of surface PS and PE in the procoagulant activity of platelet-EVs, EVs from control and TRAP-6-activated platelets were pretreated with PS- and PE-specific inhibitors (lactadherin and duramycin, respectively) before plasma clotting time was assessed by PPL assay.

Increased concentrations of lactadherin and duramycin reduced the procoagulant activity of EVs in a dose-dependent manner (Figure 3B, C). The procoagulant activity of EVs from control platelets was reduced to the level of EVDP when lactadherin was used at 10 nM and duramycin at 32 μM. A higher concentration of lactadherin (20 nM) was needed to block the procoagulant activity of EVs from TRAP-6-activated platelets, while 32 μM of duramycin was not sufficient to block their effect.

3.4 | EVs from activated platelets increase the activity of the prothrombinase complex

Next, we compared the ability of EVs from control and activated platelets to support thrombin generation in a TF-dependent manner [32]. Platelet-EVs, as the source of phospholipids, were added to a mix of coagulation factors (TF, FVIIa, FX, FV/Va, and FII), and thrombin generation was measured. EVs from TRAP-6-activated platelets increased the generation of thrombin more than 3-fold in comparison

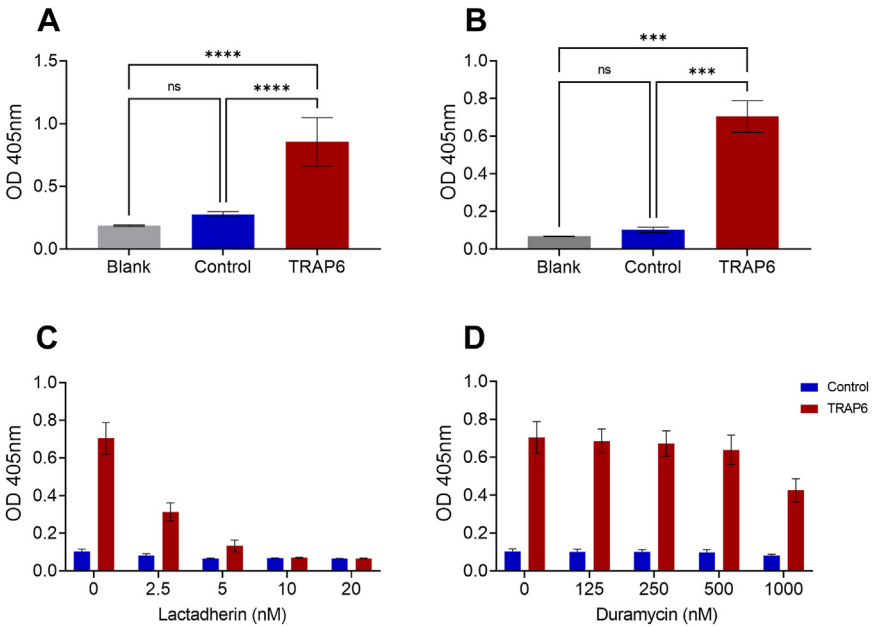

FIGURE 4 (A) Extracellular vesicles (EVs) from control and thrombin receptor activator peptide 6 (TRAP-6) activated platelets were added to a mix of coagulation factors of the extrinsic coagulation pathway (factor II, FV/FVa, FVIIa, FX, and tissue factor). Following initiation of the reaction with the addition of $CaCl_2$, thrombin generation was measured using a thrombin-specific chromogenic substrate (n = 6). (B) EVs derived from control or TRAP-6-activated platelets were added to FV/Va:FXa:FII (prothrombinase complex). Reaction was triggered with the addition of $CaCl_2$, and thrombin generation was monitored using a thrombin-specific chromogenic substrate (n = 3). (C) EVs from control platelets or platelets activated with TRAP-6 were treated with increased concentrations of lactadherin or (D) duramycin to specifically block phosphatidylserine or phosphatidylethanolamine, respectively. Thrombin generation was monitored following initiation of the reaction with the addition of $CaCl_2$ using a thrombin-specific chromogenic substrate (n = 3). ***$P < .005$, ****$P < .0001$. OD, optical density.

print & web 4C/FPO

to EVs from control platelets (OD_{405nm} = 0.854 ± 0.2 vs OD_{405nm} = 0.275 ± 0.02). The effect of EVs from TRAP-6-activated platelets on thrombin generation was dose-dependent (Supplementary Figure S8A).

To investigate the effects of platelet-EVs directly on the prothrombinase complex (ie, FII:FVa:FXa), EVs from control and TRAP-6-activated platelets were added to a mix of FXa, FV/Va, and FII, and thrombin generation was measured. As shown in Figure 4B, the activity of the prothrombinase complex was barely supported by EVs of control platelets (OD_{405nm} = 0.102 ± 0.02). In contrast, EVs from TRAP-6–activated platelets enhanced thrombin generation by more than 6-fold (OD_{405nm} = 0.704 ± 0.1, Figure 4B). Generation of thrombin by the prothrombinase complex was increased with elevated concentrations of EVs from TRAP-6-activated platelets (Supplementary Figure S8B).

To study the contribution of PS and PE displayed by platelet-EVs on the activity of the prothrombinase complex, platelet-EVs were incubated with increasing concentrations of lactadherin and duramycin. As shown in Figure 4C, blocking PS with lactadherin reduced the generation of thrombin in a dose-dependent manner. The activity of EVs from TRAP-6-activated platelets was reduced to the levels of EVs from control platelets when lactadherin was used at 10 nM. Preincubation of EVs from TRAP-6 stimulated platelets with duramycin attenuated thrombin generation. However, even a concentration as high as 1000 nM did not yield a substantial inhibition of thrombin (Figure 4D).

4 | DISCUSSION

In this study, we investigated the biomolecular composition of single or very few EVs from activated and control platelets. By means of RTM/BCA, we identified, for the first time, 3 subsets of platelet-EVs with distinct biomolecular profiles. Our analysis revealed that EVs derived from activated platelets have a more homogenous biomolecular profile rich in both proteins and lipids and carry a higher content of phospholipids compared with EVs from control platelets. To the best of our knowledge, these results present the first quantitative characterization of global biomolecular composition of single or a very small number of EVs or nano-bioparticles (up to 4 in our study) using decomposition on Raman spectra of constituent biomolecules. The observed biomolecular changes, in particular the elevated levels of phospholipids in EVs from activated platelets, were accompanied by increased procoagulant activity of EVs from TRAP-6-activated platelets, shown by an accelerated plasma coagulation and increased thrombin formation. In-depth investigation of the role of platelet-EVs in the coagulation cascade indicated that EVs from activated platelets enhanced the activity of the prothrombinase complex.

Our finding of biomolecular heterogeneity for EVs from control, unstimulated platelets poses an important question of whether all particles retained and studied in the optical trap are, in fact, EVs. The existence of an important fraction of extracellular particles has been recently introduced and discussed [40]. More specifically, many

Raman spectra of red color in Figure 1A and data points with $C_{Proteins}/C_{Lipids} > 100$ in Figure 1B characterize platelet-derived nanoparticles consisting predominantly of proteins and possessing very little lipid content. Moreover, in some extreme cases, with the value of $C_{Proteins}/C_{Lipids}$ being limited to 250 in Figure 1B (1 event for donor 1 and 7 for donor 3), we are most probably detecting protein aggregates, as lipids contribution cannot be accurately quantified here. Conversely, a few Raman spectra of blue color in Figure 1A and data points within zone C in Figure 1B characterize lipid-dominating nanoparticles with marginal, although detectable, protein content. In both cases, the observed biomolecular distribution seems to skew from the "usual" EV definition as membrane-bound vesicles carrying a myriad of biomolecules [41]. However, we note that all samples were prepared in parallel using the same protocol. Therefore, in a comparative manner, the existence of extreme biomolecular heterogeneity of EVs, including other extracellular bioparticles from unstimulated platelets, and remarkable stabilization of their biomolecular profile in the case of platelet activation constitute an important finding per se.

Platelet-EVs are abundant in plasma [16,17,42]. Higher levels of platelet-EVs were found in VTE [43,44] and other cardiovascular diseases [19,45]. Elevated plasma levels of EVs from activated platelets in plasma (identified as $CD41^{pos}/CD62P^{pos}$ EVs) are associated with VTE risk [9]. It is therefore likely that increased levels of platelet-EVs, enriched with proteins and PPLs, circulate in patients with VTE. The heterogeneity of EVs and the lack of specific EV markers, however, challenge the discovery of disease-relevant EVs and call for novel methodologies with an increased resolution and ability to identify subsets of EVs. Although challenging, RTM provides accurate information on the biochemical properties of single or very few EVs [21,22], hence suitable to detect variations of disease-relevant EV subset(s). The ability of RTM to distinguish between EVs produced by different cell lines [46] or EVs from cancer cell lines and normal cells has been demonstrated [47], as well as the identification of subsets of EVs produced by a single cell line [48].

Negatively charged phospholipids, and PS in particular, on the outer surface of activated platelets facilitate the assembly and activity of several coagulation factors [49,50], including the activity of the prothrombinase complex [51,52]. Although one would assume that platelet-EVs, and in particular EVs from activated platelets, would also facilitate the assembly and activation of the prothrombinase complex in a similar way, little work has been performed on platelet-EVs, and the reports are controversial [53,54]. By means of RTM analysis, we found that EVs from activated platelets are enriched in phospholipids. Investigation of the biological impact of such enrichment, in particular the presence of PS and PE, showed that EVs from activated platelets can accelerate plasma coagulation in a PS-dependent manner rather than PE. Furthermore, the presence of platelet-EVs as a source of phospholipids was shown to contribute specifically to the activity of the prothrombinase complex.

We presented a novel global biomolecular characterization of platelet-EVs and found that the content of lipids and phospholipids is affected by the activation state of parent platelets. For the first time, we investigated the biomolecular composition of a single or very few EVs from control and activated platelets in a quantitative manner using RTM/BCA. Furthermore, we found that EVs from TRAP-6-activated platelets, enriched in phospholipids, accelerated thrombin generation several-fold more effectively than EVs from control platelets and pinpointed their interaction with the coagulation system via the prothrombinase complex. Based on our results, it is tempting to suggest platelet-EVs as potential predictive and diagnostic biomarkers for different conditions with thrombotic manifestations. Our study thus calls for future investigation of the biomolecular profile of platelet-EVs isolated from plasma of patients with VTE, as well as other thrombotic conditions. In-depth analysis by RTM/BCA may identify subset(s) of EVs and other possible extracellular particles enriched with proteins and phospholipids, which may play a role in prothrombotic processes.

ACKNOWLEDGMENTS

This work was supported by the North Norwegian Regional Health Authority, grant HNF1548-20 to OS. ANK, and PNP at the Institute for Lasers, Photonics and Biophotonics acknowledge support from the office of vice president for research and economic development at the University at Buffalo.

AUTHOR CONTRIBUTIONS

E.M.G. and S.G.K. designed the study, carried out the experimental work, analyzed data, and wrote the manuscript. S.S. performed experiments, analyzed data, and contributed to the writing of the manuscript. N.L. contributed to the design of the study, performed experiments, analyzed data, and contributed to the writing of the manuscript. B.Ø. contributed to the design of the study and to the writing of the manuscript. J.M.G. performed experiments. F.S. performed experiments and contributed to the writing of the manuscript. S.B. contributed to data analysis and to the writing of the manuscript. A.N.K. and P.N.P. analyzed data and contributed to the writing of the manuscript. J.B.H. and O.G.H. conceived and contributed to the design of the study, and to the writing of the manuscript. O.S. conceived and designed the study, analyzed data, and wrote the manuscript.

DECLARATION OF COMPETING INTERESTS

There are no competing interests to disclose.

ORCID

Sergei G. Kruglik https://orcid.org/0000-0002-2945-3092
Omri Snir https://orcid.org/0000-0001-5322-0021

REFERENCES

[1] Cohen AT, Agnelli G, Anderson FA, Arcelus JI, Bergqvist D, Brecht JG, Greer IA, Heit JA, Hutchinson JL, Kakkar AK, Mottier D, Oger E, Samama MM, Spannagl M. Venous thromboembolism (VTE) in Europe. The number of VTE events and associated morbidity and mortality. *Thromb Haemost*. 2007;98:756–64.
[2] Heit JA. Epidemiology of venous thromboembolism. *Nat Rev Cardiol*. 2015;12:464–74.
[3] Becattini C, Agnelli G, Schenone A, Eichinger S, Bucherini E, Silingardi M, Bianchi M, Moia M, Ageno W, Vandelli MR, Grandone E,

Prandoni P. Aspirin for preventing the recurrence of venous thromboembolism. *N Engl J Med*. 2012;366:1959–67.
[4] Weitz JI, Lensing AWA, Prins MH, Bauersachs R, Beyer-Westendorf J, Bounameaux H, Brighton TA, Cohen AT, Davidson BL, Decousus H, Freitas MCS, Holberg G, Kakkar AK, Haskell L, van Bellen B, Pap AF, Berkowitz SD, Verhamme P, Wells PS, Prandoni P, et al. Rivaroxaban or aspirin for extended treatment of venous thromboembolism. *N Engl J Med*. 2017;376:1211–22.
[5] Karpatkin S, Khan Q, Freedman M. Heterogeneity of platelet function. Correlation with platelet volume. *Am J Med*. 1978;64:542–6.
[6] Braekkan SK, Mathiesen EB, Njølstad I, Wilsgaard T, Størmer J, Hansen JB. Mean platelet volume is a risk factor for venous thromboembolism: the Tromsø Study, Tromsø, Norway. *J Thromb Haemost*. 2010;8:157–62.
[7] Edvardsen MS, Hansen ES, Hindberg K, Morelli VM, Ueland T, Aukrust P, Brækkan SK, Evensen LH, Hansen JB. Combined effects of plasma von Willebrand factor and platelet measures on the risk of incident venous thromboembolism. *Blood*. 2021;138:2269–77.
[8] Edvardsen MS, Hindberg K, Hansen ES, Morelli VM, Ueland T, Aukrust P, Brækkan SK, Evensen LH, Hansen JB. Plasma levels of von Willebrand factor and future risk of incident venous thromboembolism. *Blood Adv*. 2021;5:224–32.
[9] Snir O, Wilsgård L, Latysheva N, Wahlund CJE, Braekkan SK, Hindberg K, Hansen JB. Plasma levels of platelet-derived microvesicles are associated with risk of future venous thromboembolism. *J Thromb Haemost*. 2022;20:899–908.
[10] Zwaal RF, Schroit AJ. Pathophysiologic implications of membrane phospholipid asymmetry in blood cells. *Blood*. 1997;89:1121–32.
[11] Reddy EC, Rand ML. Procoagulant phosphatidylserine-exposing platelets in vitro and in vivo. *Front Cardiovasc Med*. 2020;7:15.
[12] Biró E, Akkerman JW, Hoek FJ, Gorter G, Pronk LM, Sturk A, Nieuwland R. The phospholipid composition and cholesterol content of platelet-derived microparticles: a comparison with platelet membrane fractions. *J Thromb Haemost*. 2005;3:2754–63.
[13] Morel O, Toti F, Hugel B, Bakouboula B, Camoin-Jau L, Dignat-George F, Freyssinet JM. Procoagulant microparticles: disrupting the vascular homeostasis equation? *Arterioscler Thromb Vasc Biol*. 2006;26:2594–604.
[14] Heijnen HF, Schiel AE, Fijnheer R, Geuze HJ, Sixma JJ. Activated platelets release two types of membrane vesicles: microvesicles by surface shedding and exosomes derived from exocytosis of multivesicular bodies and alpha-granules. *Blood*. 1999;94:3791–9.
[15] Sinauridze EI, Kireev DA, Popenko NY, Pichugin AV, Panteleev MA, Krymskaya OV, Ataullakhanov FI. Platelet microparticle membranes have 50- to 100-fold higher specific procoagulant activity than activated platelets. *Thromb Haemost*. 2007;97:425–34.
[16] van der Zee PM, Biró E, Ko Y, de Winter RJ, Hack CE, Sturk A, Nieuwland R. P-selectin- and CD63-exposing platelet microparticles reflect platelet activation in peripheral arterial disease and myocardial infarction. *Clin Chem*. 2006;52:657–64.
[17] Brisson AR, Tan S, Linares R, Gounou C, Arraud N. Extracellular vesicles from activated platelets: a semiquantitative cryo-electron microscopy and immuno-gold labeling study. *Platelets*. 2017;28:263–71.
[18] Suades R, Padro T, Alonso R, Mata P, Badimon L. High levels of TSP1+/CD142+ platelet-derived microparticles characterise young patients with high cardiovascular risk and subclinical atherosclerosis. *Thromb Haemost*. 2015;114:1310–21.
[19] Hartopo AB, Puspitawati I, Gharini PP, Setianto BY. Platelet microparticle number is associated with the extent of myocardial damage in acute myocardial infarction. *Arch Med Sci*. 2016;12:529–37.
[20] Tatischeff I, Larquet E, Falcon-Perez JM, Turpin P-Y, Kruglik SG. Fast characterisation of cell-derived extracellular vesicles by nanoparticles tracking analysis, cryo-electron microscopy, and Raman tweezers microspectroscopy. *J Extracellular Vesicles*. 2012;1.
[21] Kruglik SG, Royo F, Guigner JM, Palomo L, Seksek O, Turpin PY, Tatischeff I, Falcón-Pérez JM. Raman tweezers microspectroscopy of circa 100 nm extracellular vesicles. *Nanoscale*. 2019;11:1661–79.
[22] Bordanaba-Florit G, Royo F, Kruglik SG, Falcón-Pérez JM. Using single-vesicle technologies to unravel the heterogeneity of extracellular vesicles. *Nat Protoc*. 2021;16:3163–85.
[23] Enciso-Martinez A, van der Pol E, Lenferink ATM, Terstappen L, van Leeuwen TG, Otto C. Synchronized Rayleigh and Raman scattering for the characterization of single optically trapped extracellular vesicles. *Nanomedicine*. 2020;24:102109.
[24] Enciso-Martinez A, Van Der Pol E, Hau CM, Nieuwland R, Van Leeuwen TG, Terstappen L, Otto C. Label-free identification and chemical characterisation of single extracellular vesicles and lipoproteins by synchronous Rayleigh and Raman scattering. *J Extracell Vesicles*. 2020;9:1730134.
[25] Ramberg C, Jamaly S, Latysheva N, Wilsgård L, Sovershaev T, Snir O, Hansen JB. A modified clot-based assay to measure negatively charged procoagulant phospholipids. *Sci Rep*. 2021;11:9341.
[26] Kuzmin AN, Pliss A, Kachynski AV. Biomolecular component analysis of cultured cell nucleoli by Raman microspectrometry. *J Raman Spectrosc*. 2013;44:198–204.
[27] Kuzmin AN, Pliss A, Prasad PN. Ramanomics: new omics disciplines using micro Raman spectrometry with biomolecular component analysis for molecular profiling of biological structures. *Biosensors (Basel)*. 2017;7:52.
[28] Lita A, Kuzmin AN, Pliss A, Baev A, Rzhevskii A, Gilbert MR, Larion M, Prasad PN. Toward single-organelle lipidomics in live cells. *Anal Chem*. 2019;91:11380–7.
[29] Pliss A, Kuzmin AN, Lita A, Kumar R, Celiku O, Atilla-Gokcumen GE, Gokcumen O, Chandra D, Larion M, Prasad PN. A single-organelle optical omics platform for cell science and biomarker discovery. *Anal Chem*. 2021;93:8281–90.
[30] Hemker HC, Giesen P, Al Dieri R, Regnault V, de Smedt E, Wagenvoord R, Lecompte T, Beguin S. Calibrated automated thrombin generation measurement in clotting plasma. *Pathophysiol Haemost Thromb*. 2003;33:4–15.
[31] Ramberg C, Wilsgard L, Latysheva N, Braekkan SK, Hindberg K, Sovershaev T, Snir O, Hansen JB. Plasma procoagulant phospholipid clotting time and venous thromboembolism risk. *Res Pract Thromb Haemost*. 2021;5:e12640.
[32] Østerud B, Latysheva N, Schoergenhofer C, Jilma B, Hansen JB, Snir O. A rapid, sensitive, and specific assay to measure TF activity based on chromogenic determination of thrombin generation. *J Thromb Haemost*. 2022;20:866–76.
[33] Feingold KR. Introduction to lipids and lipoproteins. In: Feingold KR, Anawalt B, Blackman MR, Boyce A, Chrousos G, Corpas E, de Herder WW, Dhatariya K, Dungan K, Hofland J, Kalra S, Kaltsas G, Kapoor N, Koch C, Kopp P, Korbonits M, Kovacs CS, Kuohung W, Laferrere B, Levy M, et al., eds. *Endotext*. South Dartmouth (MA): MDText.com, Inc; 2000.
[34] Aatonen MT, Ohman T, Nyman TA, Laitinen S, Grönholm M, Siljander PR. Isolation and characterization of platelet-derived extracellular vesicles. *J Extracell Vesicles*. 2014;3.
[35] Mutlu A, Gyulkhandanyan AV, Freedman J, Leytin V. Concurrent and separate inside-out transition of platelet apoptosis and activation markers to the platelet surface. *Br J Haematol*. 2013;163:377–84.
[36] Wei H, Malcor JM, Harper MT. Lipid rafts are essential for release of phosphatidylserine-exposing extracellular vesicles from platelets. *Sci Rep*. 2018;8:9987.
[37] White JG, Rao GH, Gerrard JM. Effects of the Ionophore A23187 on blood platelets I. Influence on aggregation and secretion. *Am J Pathol*. 1974;77:135–49.
[38] Swords NA, Tracy PB, Mann KG. Intact platelet membranes, not platelet-released microvesicles, support the procoagulant activity of adherent platelets. *Arterioscler Thromb*. 1993;13:1613–22.

[39] Tavoosi N, Davis-Harrison RL, Pogorelov TV, Ohkubo YZ, Arcario MJ, Clay MC, Rienstra CM, Tajkhorshid E, Morrissey JH. Molecular determinants of phospholipid synergy in blood clotting. *J Biol Chem*. 2011;286:23247–53.

[40] Jeppesen DK, Fenix AM, Franklin JL, Higginbotham JN, Zhang Q, Zimmerman LJ, Liebler DC, Ping J, Liu Q, Evans R, Fissell WH, Patton JG, Rome LH, Burnette DT, Coffey RJ. Reassessment of exosome composition. *Cell*. 2019;177:428–45.e18.

[41] Zaborowski MP, Balaj L, Breakefield XO, Lai CP. Extracellular vesicles: composition, biological relevance, and methods of study. *Bioscience*. 2015;65:783–97.

[42] György B, Szabó TG, Pásztói M, Pál Z, Misják P, Aradi B, László V, Pállinger E, Pap E, Kittel A, Nagy G, Falus A, Buzás EI. Membrane vesicles, current state-of-the-art: emerging role of extracellular vesicles. *Cell Mol Life Sci*. 2011;68:2667–88.

[43] Bal L, Ederhy S, Di Angelantonio E, Toti F, Zobairi F, Dufaitre G, Meuleman C, Mallat Z, Boccara F, Tedgui A, Freyssinet JM, Cohen A. Factors influencing the level of circulating procoagulant microparticles in acute pulmonary embolism. *Arch Cardiovasc Dis*. 2010;103:394–403.

[44] Bucciarelli P, Martinelli I, Artoni A, Passamonti SM, Previtali E, Merati G, Tripodi A, Mannucci PM. Circulating microparticles and risk of venous thromboembolism. *Thromb Res*. 2012;129:591–7.

[45] Li S, Wei J, Zhang C, Li X, Meng W, Mo X, Zhang Q, Liu Q, Ren K, Du R, Tian H, Li J. Cell-derived microparticles in patients with type 2 diabetes mellitus: a systematic review and meta-analysis. *Cell Physiol Biochem*. 2016;39:2439–50.

[46] Penders J, Nagelkerke A, Cunnane EM, Pedersen SV, Pence IJ, Coombes RC, Stevens MM. Single particle automated Raman trapping analysis of breast cancer cell-derived extracellular vesicles as cancer biomarkers. *ACS Nano*. 2021;15:18192–205.

[47] Lee W, Nanou A, Rikkert L, Coumans FAW, Otto C, Terstappen L, Offerhaus HL. Label-free prostate cancer detection by characterization of extracellular vesicles using Raman spectroscopy. *Anal Chem*. 2018;90:11290–6.

[48] Smith ZJ, Lee C, Rojalin T, Carney RP, Hazari S, Knudson A, Lam K, Saari H, Ibañez EL, Viitala T, Laaksonen T, Yliperttula M, Wachsmann-Hogiu S. Single exosome study reveals subpopulations distributed among cell lines with variability related to membrane content. *J Extracell Vesicles*. 2015;4:28533.

[49] Medfisch SM, Muehl EM, Morrissey JH, Bailey RC. Phosphatidylethanolamine-phosphatidylserine binding synergy of seven coagulation factors revealed using Nanodisc arrays on silicon photonic sensors. *Sci Rep*. 2020;10:17407.

[50] Wang J, Yu C, Zhuang J, Qi W, Jiang J, Liu X, Zhao W, Cao Y, Wu H, Qi J, Zhao RC. The role of phosphatidylserine on the membrane in immunity and blood coagulation. *Biomark Res*. 2022;10:4.

[51] Wood JP, Silveira JR, Maille NM, Haynes LM, Tracy PB. Prothrombin activation on the activated platelet surface optimizes expression of procoagulant activity. *Blood*. 2011;117:1710–8.

[52] Haynes LM, Bouchard BA, Tracy PB, Mann KG. Prothrombin activation by platelet-associated prothrombinase proceeds through the prethrombin-2 pathway via a concerted mechanism. *J Biol Chem*. 2012;287:38647–55.

[53] Sims PJ, Wiedmer T, Esmon CT, Weiss HJ, Shattil SJ. Assembly of the platelet prothrombinase complex is linked to vesiculation of the platelet plasma membrane. Studies in Scott syndrome: an isolated defect in platelet procoagulant activity. *J Biol Chem*. 1989;264:17049–57.

[54] Aleman MM, Gardiner C, Harrison P, Wolberg AS. Differential contributions of monocyte- and platelet-derived microparticles towards thrombin generation and fibrin formation and stability. *J Thromb Haemost*. 2011;9:2251–61.

SUPPLEMENTARY MATERIAL

The online version contains supplementary material available at https://doi.org/10.1016/j.jtha.2024.01.004.